JOC The Journal of Organic Chemistry

Article

pubs.acs.org/joc

Concise Total Synthesis and Stereochemical Analysis of Tetraponerines T3 and T4

Irene Bosque, José C. González-Gómez,* Albert Guijarro,* Francisco Foubelo, and Miguel Yus

Departamento de Química Orgánica, Facultad de Ciencias and Instituto de Síntesis Orgánica (ISO), Universidad de Alicante, Apdo. 99, 03080 Alicante, Spain

Supporting Information

ABSTRACT: An efficient stereocontrolled preparation of tetraponerines **T3** and **T4** is detailed. The sequence takes advantage of two consecutive stereoselective aminoallylations of appropriate aldehydes with chiral *tert*-butanesulfinamide and *in situ* generated allyl indium species. The absolute configuration of the carbon stereogenic center at the aminal moiety is thermodynamically controlled. This was ascertained on the basis of an exhaustive DFT configurational study of tetraponerines, which fulfils the lack of detailed structural information for these systems. It was found that the *trans-transoid*-configuration of the AB rings is the most stable geometry for **T3** and **T4**. However, the C ring prefers a *cis*-configuration in **T3** (*ttc*-**T3**) and a *trans*-fusion in **T4** (*ttt*-**T4**). Regarding their dynamic behavior, low activation barriers were found by DFT calculations for the inversion of the nitrogen at the indolizidine framework, allowing rapid equilibration between the major configurations (*ttc* and *ttt*) in **T3** and **T4**.

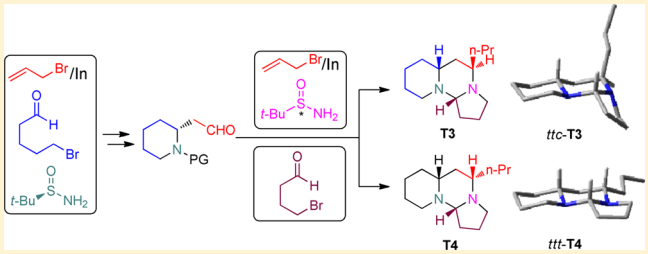

INTRODUCTION

In 1987 Braekman et al. reported the isolation and the structure determination of tetraponerines, a family of alkaloids that Pseudomyrmecine ants of the genus *Tetraponera* segregate against their enemies.[1] These tricyclic alkaloids, named tetraponerines **T1**−**T8**, possess a singular aminal moiety and can be divided into two structural families according to the size of the ring A (Figure 1). Interestingly, some experimental

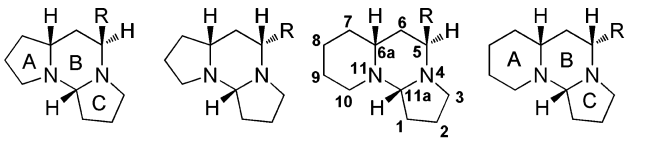

Figure 1. Structures of tetraponerines **T1**−**T8**.

evidence has been found to support two different pathways for the biosynthesis of the two tetraponerine skeletons.[2,3] In each family, the compounds differ from each other by the length of the alkyl chain (propyl or pentyl) and/or by the configuration at C_5. The structure and relative configuration of the major component of the mixture of these eight toxic alkaloids, (+)-**T8**, was determined by X-ray diffraction analysis,[1] and its absolute configuration was confirmed by enantioselective synthesis.[4] Although the original structures proposed for **T3**, **T5**, **T6**, and **T7** were wrong, extensive spectroscopic and circular dichroism studies allowed the correction of these structures.[5,6]

Tetraponerines act as paralyzing venoms that are used as chemical warfare by the host species, and consequently it was earlier found that they exhibit insecticidal activity.[1] Recent studies categorize them as efficient inhibitors of a range of nAChRs (nicotinic acetylcholine receptors).[7] More recently, it has also been found that these molecules and some analogues possess cytotoxic activity.[8] The unprecedented tricyclic skeleton along with the interest in their biological activities have made them attractive targets for total synthesis.[9] Despite these elegant and creative synthetic approaches, efficient syntheses of this family of alkaloids that can be easily modified to prepare biologically active analogues are still desirable. Moreover, insight into the configurational spectrum of tetraponerines could be important to understand their mode of action in any activity displayed as well as to perform a rationale search of structure−activity for tetraponerine derived compounds. In this context, we present herein a concise divergent synthesis of tetraponerines **T3** and **T4**, as well as their configurational and conformational analysis using DFT calculations.

RESULTS AND DISCUSSION

Upon biosynthetic studies, **T8** was subjected to chemical degradation, and it was found that N_{11}−C_{11a} could be selectively cleaved by catalytic hydrogenation in acidic media, most likely through the corresponding iminium ion.[2] Notably, the absolute stereochemistry at the aminal center (C_{11a}) of all

Received: September 18, 2012
Published: October 23, 2012

natural tetraponerines is the same regardless the configuration (R/S) at C_5. With this in mind, we speculated that the configuration at the aminal center of natural tetraponerines could be thermodynamically controlled by equilibration between the most stable aminals and the corresponding open iminium form. On the basis of this hypothesis we anticipated that rings B and C of tetraponerines **T3** and **T4** could be formed, with the right stereochemistry at C_{11a}, by reaction of 4-bromobutanal[10] with the corresponding diamines. Relying on our indium stereoselective aminoallylation of aldehydes,[11] we traced back the synthesis of diamine derivatives to 5-bromopentanal, chiral *tert*-butanesulfinamide, and *in situ* generated allyl indium species (Scheme 1). Hence we

Scheme 1. Retrosynthetic Analysis of Tetraponerines T3 and T4

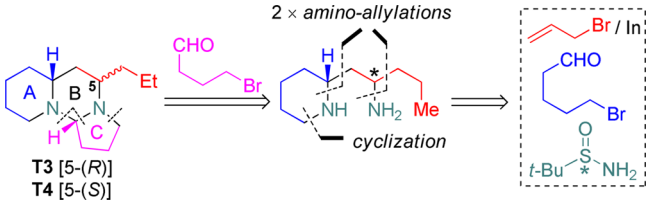

envisioned a protocol where a protected 2-allylpiperidine is formed from 5-bromopentanal, transformed into the corresponding aldehyde, and submitted to a second aminoallylation to afford the desired diamines. Importantly, both required diastereomeric diamines could be available by using either (S_S)-*tert*-butanesulfinamide or its enantiomer.

As depicted in Scheme 2, our synthesis commenced with an efficient preparation of the 2-allylpiperidine derivative **1a**.[12]

Scheme 2. Divergent Stereoselective Synthesis of Diamine Derivatives 3a and 3b

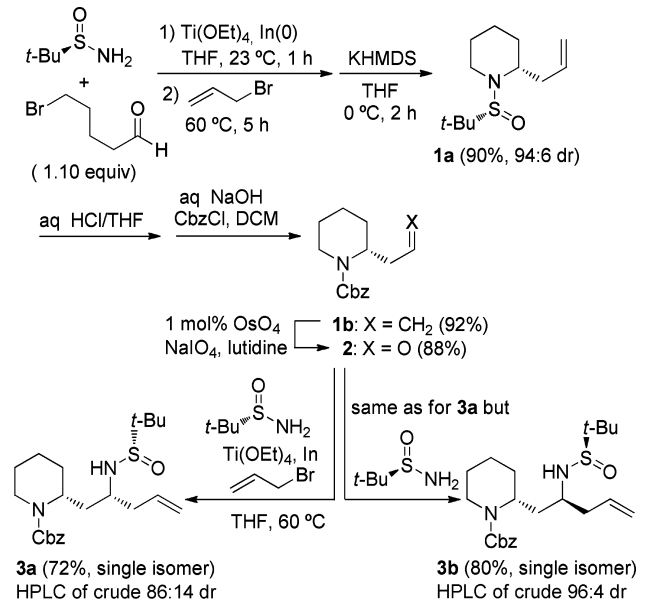

One-pot transformation of **1a** into **1b** was followed by oxidative cleavage of the olefinic double bond using a modified Johnson-Lemieux oxidation.[13] Aminoallylation of aldehyde **2** using our indium-mediated protocol with (S_S)-*tert*-butanesulfinamide[11] took place smoothly with moderate diasteroselectivity (86:14 dr, where 14% is the sum of other isomers). More importantly, compound **3a** was isolated in 72% yield as a single isomer after column purification. When aldehyde **2** was submitted to the same reaction conditions, but using (R_S)-*tert*-butanesulfinamide, better diasteroselection was observed for compound **3b** (96:4 dr), which was isolated as a single isomer in 80% yield after column purification. Remarkably, even for the mismatched case (**3a**), the stereoinduction of the chiral sulfinyl group exceeds the effect of the stereocenter at the piperidine ring, which was crucial to access both required configurations at the homoallylic stereocenter. Moreover, the iterative use of the stereoselective aminoallylation procedure (initially to prepare **1a** in 94:6 dr) resulted in an enantiomeric enhancement that allowed the isolation of **3a** or **3b** in more than 99:1 er.

With an efficient method in hand to prepare diamine derivatives **3a** and **3b** with high enantiomeric purity, the free diamines were prepared by aqueous acidic removal of the chiral auxiliary followed by catalytic hydrogenation of the olefin moiety with concomitant removal of the carbamate group (Scheme 3). The crude diamines were treated with 4-

Scheme 3. Endgame in the Synthesis of T3 and T4

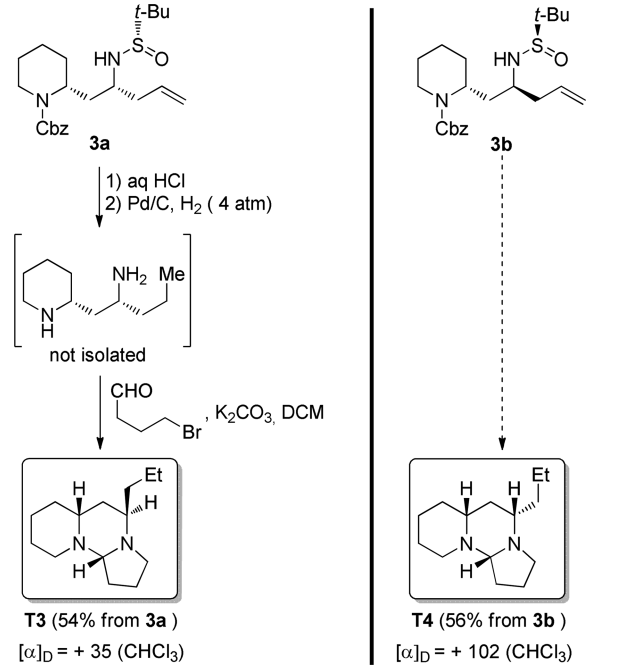

bromobutanal in the presence of K_2CO_3 to obtain tetraponerines **T3** and **T4**, respectively, in good overall yield. Spectral and physical data for these compounds (e.g., ^1H and ^{13}C NMR, IR, optical rotation) were in good agreement with those reported in the literature for natural[5] and synthetic samples.[9b] Importantly, when the biological activity of tetraponerine analogues was recently evaluated, the long-chain derivatives at C_5 systematically displayed the lowest IC_{50} values.[7,8] In this context, the synthesis described here could be easily modified to enlarge the chain at C_5 of **T3** or **T4** by cross-metathesis of intermediates **3a** or **3b** with the corresponding terminal alkenes.

As we mentioned before, our synthetic approach to tetraponerines **T3** and **T4** relied on the hypothesis that the natural alkaloids are the most stable aminals possible. We have not found any comprehensive study on the conformational and

dx.doi.org/10.1021/jo302045y | J. Org. Chem. 2012, 77, 10340−10346

configurational analysis of tetraponerines, so in order to fulfill the lack of detailed structural information, we did an exhaustive computational study of all of the different stereoisomeric configurations that, in principle, are conceivable using this as well as other synthetic methodologies. For that purpose, a few remarks on the stereochemical nomenclature and notation used are pertinent. Concerning the nitrogen atoms, the relevant configurational descriptors of the pyramidal nitrogen were specifically defined, in coherence with the calculation inputs. Until now, this task has been always overlooked, probably on the basis of the expected low nitrogen inversion barriers. Thus, we speak of configuration of the pyramidal nitrogen regardless of its inversion barrier. Both **T3** and **T4** share a bicyclic quinolizidine (rings AB, Figure 1) as well as an indolizidine (rings BC, Figure 1) fragment. We used as a starting anchor point the configuration of C_{6a}, which is invariably *R* in these natural products. The configuration of the nearest nitrogen, N_{11}, defines the type of ring fusion of the AB fragment, either *cis*- or *trans*-. Next, the relative stereochemistry of the quinolizidine and indolizidine frameworks (i.e., the rings AB and BC) was defined as either *cisoid* or *transoid*. Finally the indolizidine ring fusion BC is again defined as either *cis* or *trans*. Figure 2 exemplifies it for some important configurations of **T3** and **T4**.

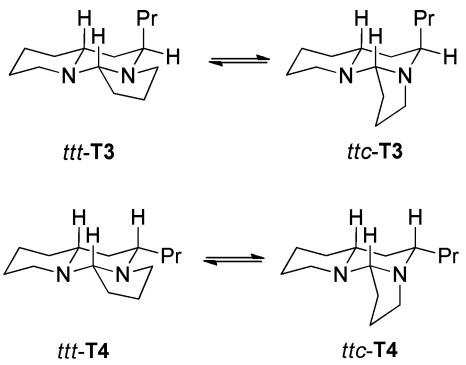

Figure 2. Stereochemical descriptors of **T3**, **T4** stereoisomers. As an example, the *trans-transoid-trans*-**T3** and -**T4** (*ttt*-**T3** and *ttt*-**T4**) and the corresponding *trans-transoid-cis*-**T3** and -**T4** (*ttc*-**T3** and *ttc*-**T4**) are represented.

When the AB ring fusion is *cis*-, the quinolizidine framework exists as an equilibrium mixture of two well-defined conformers (just as in *cis*-decalin). These have been named here as series 1 and 2, which interconvert by simple ring flip and are illustrated in Figure 3 in the case of *cis-cisoid-cis*-**T4** (*ccc*-**T4** ⇆ *ccc*2-**T4**). In general, other local conformations (e.g., the envelope in the pyrrolidine ring) were imposed by the rest of the structure. Finally, the *n*-propyl side chain was always found to accommodate in an extended conformation gauche to the C_6.[14] Altogether, these stereochemical motifs defined precisely

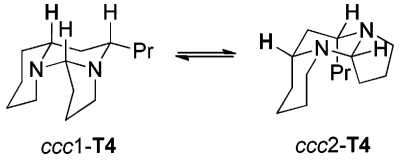

Figure 3. Conformations of the *cis*- series 1 and 2 exchanging by ring flip. By definition, H_{6a} (boldface) is axial in ring B in series 1 and equatorial in series 2.

the conformational and configurational space of this family of compounds.

The results of this DFT study are represented in Charts 1 and 2.[15,16] The hypothesis of a thermodynamic control of the reaction is sound. For both **T3** and **T4**, the most stable geometry corresponds to the *trans-transoid*-configurations of the AB rings, while the C ring prefers a *cis*-configuration in **T3** (*ttc*-**T3**, ΔE = −0.38 kcal mol^{-1}, population 66%), closely followed by the opposite C ring fusion (*ttt*-**T3**, ΔE = 0 kcal mol^{-1}, population 33%). The third configuration in order of stability is a **T3** diastereomer with an inverted configuration at C_{11a} and an expected hypothetical population of less than 1% in the mixture (i.e., the *ctt*2-**T3**, ΔE = 2.34 kcal mol^{-1}, population 0.47%). For **T4**, the configurational spectrum is dominated by the *trans*-fusion at the C ring (*ttt*-**T4**, ΔE = 0 kcal mol^{-1}, population 95%), with only a minor population of <5% of the *cis*-isomer at the C ring (i.e., the *ttc*-**T4**, ΔE = 1.81 kcal mol^{-1}, population 4.5%).

The reason for the reported order of stabilities are a combination of strain, steric, and to a lesser extent, electronic effects. Among the last ones, the anomeric effect in the **T3**-**4** system may be described as a stabilizing effect originated by hyperconjugation of one nitrogen lone pair with the empty C_{11a}−N σ^* bond of the second nitrogen, which may operate along with an alternative mechanism of dipole cancellation, expected to be less important in these systems. Depending on the relative geometric orientation of the two nitrogen atoms around C_{11a}, the possibility of none (*ccc*2-, *ctt*2-, *tcc*- and *ttt*-**T3**-**4**), one, or two (*ccc*-**T3**-**4**) anomeric interactions stabilizing the structure may arise. The effect is strongly dependent on the overlap of these two orbitals and is maximum with an antiparallel alignment between them. In general, the anomeric effect was found to be less important, and its additive effect to the overall energy is easily masked by other stronger interactions. For instance, two out of the three **T3** configurations with lower energy as well as the lowest energy configuration of **T4** have zero anomeric effects (*ttt*-**T3**-**4** and *ctt*2-**T3**). The most stable **T3** configuration (the *ttc*-**T3**) has one clear anomeric effect, but so have most of the remaining configurations. The *ccc*-**T3** configuration is the only one having two simultaneous anomeric interactions; however, it lies 6.28 kcal mol^{-1} above the minimum and is therefore not representative in practice of the **T3**.[17] The same is true for the *ccc*-**T4**, which lies 8.29 kcal mol^{-1} above the minimum. Despite this, the anomeric effect exists and is patent in the calculated geometries. It can be identified by a small but regular shortening of the donor N−C_{11a} bond and a lengthening of the acceptor N−C_{11a} bond, which is statistically consistent for both the **T3** and **T4** configurations. The C_{11a}−N average bond devoid of anomeric effects is 1.461 Å (σ = ± 0.006 Å). The average N−C_{11a} bond with anomeric shortening is 1.454 Å (σ = ± 0.005 Å), while the average bond with anomeric lengthening is 1.483 Å (σ = ± 0.008 Å).[18] We have quantitatively evaluated the magnitude of the anomeric effect by means of second order perturbation theory, estimating the donor−acceptor (bond−antibond) interactions on the NBO (Natural Bond Orbital) basis.[19] Typical stabilization energies in the 10−11 kcal mol^{-1} range were actually found for the nitrogen lone pair (donor N LP) interacting with an antiparallel carbon−nitrogen sigma antibond (acceptor C_{11a}−N σ^*). Although these are fairly typical values for an anomeric stabilization, we found that the N LP was also capable to stabilize a range of acceptor antibonds provided that they were antiperiplanar to the N LP, with

dx.doi.org/10.1021/jo302045y | J. Org. Chem. 2012, 77, 10340−10346

Chart 1. DFT Energy Profiles (ΔE Including ZPE Corrections in kcal mol^{-1}) of Local Minima for All T3 Configurations[a]

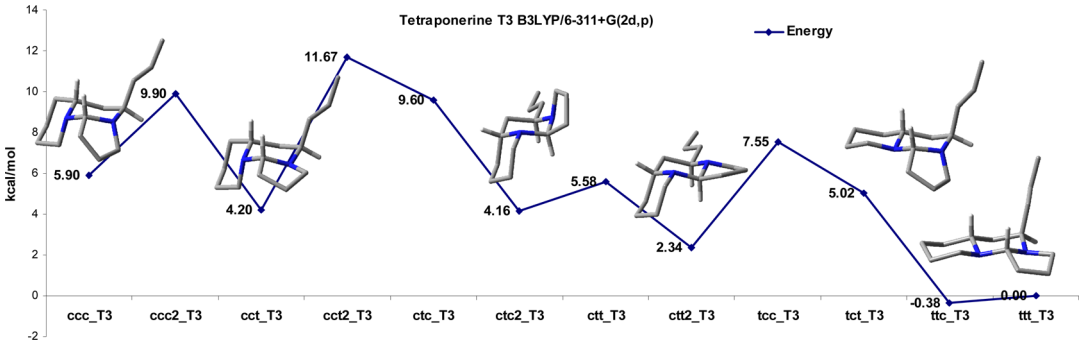

[a]The structures of the six configurations lower in energy are drawn.

Chart 2. DFT Energy Profiles (ΔE Including ZPE Corrections in kcal mol^{-1}) of Local Minima for All T4 Configurations[a]

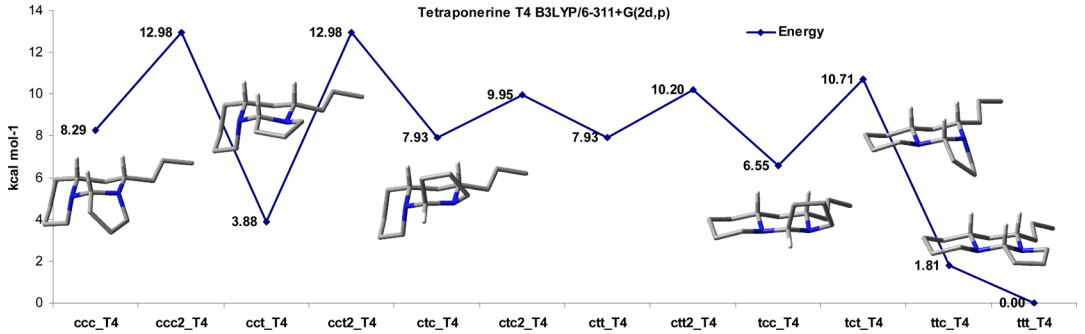

[a]The structures of the six configurations lower in energies are drawn. During geometry optimization, the *ccc*2-**T4** became *cct*2-**T4** and the *ctt*-**T4** became *ctc*-**T4**. Both are consistent with a spontaneous release of strain through nitrogen inversion at the indolizidine framework.

surprisingly high stabilization energies, that altogether may compensate or even overcome the anomeric effect in the inverted configuration (i.e., that lacking anomeric effect).[20] Among these interactions, the N LP-C−H_{ax} σ^* is historically relevant since it gives rise to the so-called Bohlmann bands in IR spectroscopy,[21] a specific C−H stretching of the axial hydrogens adjacent to the nitrogen atom.

Concerning tensional and steric effects, two important patterns of destabilization are easily identified. The methylene-methylene (or alkyl-alkyl) 1,3-diaxial interactions, as occurring in *ccc*-**T3**-**4**, *ccc*2-**T3**, *ctc*-**T3**, *ctc*2-**T4**, *ctt*2-**T4**, and *tcc*-**T3**, is one of them. The second, even more severe, is a ring B deformation from chair into other distorted conformations such as twisted boat, which occurs when a tentative *trans*-diaxial fusion with ring C is imposed, e.g., *cct*2-**T3**-**4**, *ctt*-**T3**, *tct*-**T3**-**4**.[15] None of these destabilizing elements are found in the more stable configurations of **T3** and **T4**. The main stereochemical elements of these configurations follow.[22] For **T3**, *ttt*-**T3** has a *trans*-quinolizidine type of fusion and lacks anomeric stabilization. There is a small gauche interaction between C_3 and Pr. This interaction can be avoided by nitrogen inversion at N_4, becoming then the more stable configuration, *ttc*-**T3**, at the expense of an additional 1,3-diaxial methylene interaction with only one hydrogen atom (Figure 2 and Chart 1). In addition, *ttc*-**T3** takes advantage of one anomeric stabilization between the N_4 lone pair and the empty C_{11a}−N_{11} σ^* (the calculated C_{11a}−N_4 and C_{11a}−N_{11} bond lengths are 1.455 and 1.489 Å, respectively). In the less stable *ctt*2-**T3**, there is a *cis*-quinolizidine type of fusion, but the Pr group is equatorial. The methylene C_7 is in 1,3-diaxial interaction but only with 2 hydrogens, and there is a small gauche interaction C_3 with the Pr group, as well as no anomeric effects. For **T4**, the *ttt*-**T4** has a *trans*-quinolizidine type of fusion also and no anomeric stabilization. There is a small gauche interaction between C_3 and Pr that is not relieved now by nitrogen inversion at N_4, which makes it the more stable configuration. The inverted *ttc*-**T4** has still that gauche interaction, as well as an additional 1,3-diaxial methylene interaction with only 1 hydrogen (Figure 2 and Chart 2), which seems not to be compensated by the appearance of one anomeric stabilization similar to the one described before (calculated C_{11a}−N_4 and C_{11a}−N_{11} bond lengths are 1.454 and 1.489 Å, respectively).

Finally, although the **T3** and **T4** do not interconvert spontaneously, a comparison of the intrinsic stability of both tetraponerines was done. Overall, for the theoretical interconversion **T3** ⇆ **T4**, ΔG° is −2.52 kcal mol^{-1}, meaning that the tetraponerine **T4** would account for 98.6% and the **T3** only for the remaining 1.4% of a hypothetical equilibrating mixture.[23] This issue proved to be crucial in a previous stereoselective synthesis of **T4**, the final step of which relied on a thermodynamic equilibration of the Pr group attached to a fast inverting radical at C_5.[9a]

We next focused our attention on the inversion barriers of the N_{11} (quinolizidine framework) and the N_4 (indolizidine framework). Starting from the major components of the **T3** and **T4**, the nitrogen inversion at the quinolizidine part of the molecule (i.e., at N_{11}) affords substantially more unstable configurations: *ttc*-**T3** (66%) ⇆ *ccc*-**T3** (ca. 0.0013%) and *ttt*-**T3** (33%) ⇆ *cct*-**T3** (ca. 0.020%), as well as *ttc*-**T4** (4.5%) ⇆ *ccc*-**T4** (3.7×10^{-5} %) and *ttt*-**T4** ⇆ *cct*-**T4** (ca. 0.15%). These inverted configurations are unstable enough to prevent (or at least to complicate very much) experimental determination of

dx.doi.org/10.1021/jo302045y | J. Org. Chem. 2012, 77, 10340−10346

the equilibria and have little practical relevance. However, this is not the case for the indolizidine fragment. The inversion at the N_4 exchanges two substantially populated configurations, particularly in the case of **T3**: *ttc*-**T3** (66%) ⇆ *ttt*-**T3** (33%) and *ttt*-**T4** (95%) ⇆ *ttc*-**T4** (4.5%). The calculated activation barriers for these two processes are reported in Figure 4 and

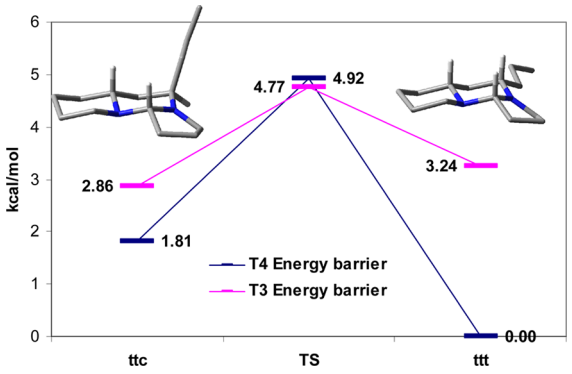

Figure 4. Calculated activation barriers for N_4 inversion in **T3** (ΔE = 1.90 kcal mol^{-1}) and **T4** (ΔE = 4.92 kcal mol^{-1}) at the B3LYP/6-311+G (2d,p) level. Notice the trigonal planar geometry at the inverting nitrogen; ν = 126.27 *i* cm^{-1} for the transition state TS-**T3** (top left) and ν = 163.64 *i* cm^{-1} for the transition state TS-**T4** (top right).

correspond to the processes drawn in Figure 2. In both cases, at the transition state the nitrogen displays a trigonal planar geometry. Visual examination of the imaginary frequency mode passing through the transition state confirmed the correct nature of the calculated saddle points TS-**T3**-**4**. Since the barriers encountered are low, a rapid interconversion between these two configurations for each tetraponerine is expected.[24]

CONCLUSION

The iterative use of stereoselective aminoallylation of aldehydes with chiral *tert*-butanesulfinamide and *in situ* generated allyl indium species has been successfully applied to the synthesis of tetraponerines **T3** and **T4**. The formation of rings B and C was achieved by reaction of the corresponding enantioenriched free diamines with 4-bromobutanal, obtaining the desired aminals with the right stereochemistry at the aminal center (C_{11a}). An exhaustive configurational analysis of **T3** and **T4** by DFT calculations revealed that they are mainly populated (>99%) by isomers with the *trans-transoid*-configuration at the AB rings, which clearly supports the hypothesis of a thermodynamic control of the stereochemistry at the aminal center. This study also shows that the C ring prefers a *cis*-configuration in **T3** (*ttc*-**T3**) and a *trans*-fusion in **T4** (*ttt*-**T4**), although both are in rapid equilibration with their respective second most populated configurations (i.e., *ttt*-**T3** and *ttc*-**T4**) given the low activation barriers calculated for the nitrogen inversion at the indolizidine framework.

EXPERIMENTAL SECTION

General Remarks. (R_S)-*tert*-Butanesulfinamide and its enantiomer were a gift of Medalchemy (>99% ee by chiral HPLC on a Chiracel AS column, 90:10 hexane/*i*-PrOH, 1.2 mL/min, λ = 222 nm). TLC was performed on silica gel 60 F_{254} using aluminum plates and visualized with phosphomolybdic acid (PMA) stain. Flash chromatography was carried out on handpacked columns of silica gel 60 (230−400 mesh). Melting points are uncorrected. Optical rotations were measured using a polarimeter with a thermally jacketted 5 cm cell at approximately 20 °C and concentrations (c) are given in g/100 mL. Infrared analysis was performed with a spectrophotometer equipped with an ATR component; wavenumbers are given in cm^{-1}. Mass spectra (EI) were obtained at 70 eV, and fragment ions are in m/z with relative intensities (%) in parentheses. HRMS analyses were also carried out in the electron impact mode (EI) at 70 eV using a quadrupole mass analyzer. GC analyses were obtained with an HP-5 column (30 m × 0.25 mm, i.d. × 0.25 μm) and an EI (70 EV) detector. The temperature program was as follows: hold at 60 °C for 3 min, ramp from 60 to 270 °C at 15 °C/min, hold at 270 °C for 10 min.

^{1}H NMR spectra were recorded at 300 or 400 MHz for ^{1}H NMR and 75 or 100 MHz for ^{13}C NMR, using $CDCl_3$ or C_6D_6 as solvents and TMS as internal standard (0.00 ppm). The data is reported as (s = singlet, d = doublet, t = triplet, m = multiplet or unresolved, br s = broad signal, coupling constant(s) in Hz, integration). ^{13}C NMR spectra were recorded with ^{1}H-decoupling at 100 MHz and referenced to $CDCl_3$ at 77.16 ppm or to C_6D_6 at 128.06 ppm. DEPT-135 experiments were performed to assign CH, CH_2 and CH_3.

(*R*)-2-Allyl-1-(benzyloxicarbonyl)piperidine (1b). An aqueous 6 M solution of HCl (1.5 mL, 9.00 mmol) was added dropwise to a solution of **1a**[12] (687 mg, 3.00 mmol) in dry THF (3 mL) at 0 °C under Ar. The solution was allowed to reach 23 °C and was stirred for 1.5 h. After the mixture cooled to 0 °C, an aqueous 2 M solution of NaOH (14 mL, 27.00 mmol) was added dropwise, and the resulting mixture was stirred at the same temperature. After 5 min, a solution of benzyloxycarbonyl chloride (515 μL, 3.60 mmol) in CH_2Cl_2 (11 mL) was added to the stirred solution. The resulting mixture was then allowed to reach 23 °C and was stirred for 3 h. The reaction mixture was extracted with EtOAc (3 × 20 mL), and the combined organic layers were washed with H_2O, dried over $MgSO_4$, filtered, and concentrated under reduced pressure. The residue was purified by column chromatograpy (95:5 hexane/EtOAc) to provide the desired product as a colorless oil (715 mg, 92%). R_f = 0.26 (9:1 hexane/EtOAc); $[\alpha]^{20}_D$ = +44 (c 0.498 in $CHCl_3$); ^{1}H NMR (300 MHz, $CDCl_3$) δ 7.37−7.28 (m, 5H), 5.71 (td, J = 16.5, 7.3 Hz, 1H), 5.19−4.95 (m, 4H), 4.37 (br s, 1H), 4.05 (d, J = 12.3 Hz, 1H), 2.86 (td, J = 12.8, 2.5 Hz, 1H), 2.43 (dddd, J = 10.5, 7.4, 2.4, 1.2 Hz, 1H), 2.25 (dt, J = 14.0, 7.1 Hz, 1H), 1.73 −1.54 (m, 5H), 1.54 −1.31 (m, 1H); ^{13}C NMR (101 MHz, $CDCl_3$) δ 155.7 (C), 137.2 (C), 135.4 (CH), 128.6 (CH), 128.0 (CH), 127.9 (CH), 117.0 (CH_2), 67.0 (CH_2), 50.5 (CH), 39.4 (CH_2), 34.6 (CH_2), 27.7 (CH_2), 25.6 (CH_2), 18.9 (CH_2); IR (ATR) ν 3035, 2937, 2859, 1691, 1641, 1445, 1421, 1258, 1240 cm^{-1}; LRMS (EI) m/z (%) 259 (M^+, 0.1), 219 (19), 218 (100), 175 (32), 174 (100), 92 (40), 91 (100), 65 (35), 55 (20); HRMS (EI) m/z calcd for $C_{16}H_{21}NO_2$ 259.1572, found 259.1601.

(*R*)-1-(Benzyloxicarbonyl)-2-(2-oxoethyl)piperidine (2). To a solution of **1b** (684 mg, 2.64 mmol) in 1,4-dioxane/H_2O (3:1, 27 mL) were successively added 2,6-lutidine (615 μL, 5.28 mmol), $NaIO_4$ (2.30 g, 10.56 mmol), and a solution of OsO_4 in *t*-BuOH (2.5% w/w in *t*-BuOH, 260 μL). The mixture was stirred at 23 °C for 1.5 h before being quenched with water (20 mL). The mixture was extracted with EtOAc (3 × 20 mL), and the collected organic layers were washed with H_2O, dried over $MgSO_4$, filtered, and concentrated under reduced pressure. The residue was purified by column chromatograpy (4:1 hexane/EtOAc) to provide the pure product as a colorless oil (610 mg, 88%). R_f = 0.30 (7:3 hexane/EtOAc); $[\alpha]^{20}_D$ = +42 (c 0.34 in $CHCl_3$); ^{1}H NMR (300 MHz, $CDCl_3$) δ 9.71 (s, 1H), 7.42−7.29 (m, 5H), 5.12 (s, 2H), 4.93 (dd, J = 13.0, 6.9 Hz, 1H), 4.08 (d, J = 13.1 Hz, 1H), 2.85 (t, J = 13.0 Hz, 1H), 2.75 (ddd, J = 15.6, 8.1, 3.0 Hz, 1H), 2.60 (ddd, J = 15.7, 6.9, 2.0 Hz, 1H), 1.81 −1.32 (m, 6H); ^{13}C NMR (101 MHz, $CDCl_3$) δ 200.7 (CH), 155.4 (C), 136.7 (C), 128.6 (CH), 128.2 (CH), 128.0 (CH), 67.4 (CH_2), 46.3 (CH), 44.6 (CH_2), 39.8 (CH_2), 28.8 (CH_2), 25.3 (CH_2), 19.0 (CH_2); IR (ATR) ν 3026, 2939, 2860, 2731, 1721, 1687, 1445, 1418, 1257, 1238 cm^{-1}; LRMS (EI) m/z (%) 261 (M^+, 3), 233 (27), 218 (20), 175 (13), 174 (100), 170 (18), 126 (27), 108 (20), 92 (29), 91 (100), 65 (30), 55 (13); HRMS (EI) m/z calcd for $C_{15}H_{19}NO_3$ 261.1365, found 261.1351.

(2*R*,2′*S*,*S*$_S$)-1-(Benzyloxicarbonyl)-2-[2′-*tert*-(butylsulfinamide)-4′-pentenyl]piperidine (3a). To a dry flask were added (S_S)-

dx.doi.org/10.1021/jo302045y | J. Org. Chem. 2012, 77, 10340−10346

tert-butanesulfinamide (220 mg, 1.82 mmol) and indium powder (259 mg, 2.27 mmol) under Ar. Then was added a solution of compound **2** (496 mg, 1.90 mmol) in dry THF (4.5 mL) followed by $Ti(OEt)_4$ (818 μL, 3.64 mmol), and the reaction mixture was stirred under Ar for 1 h at 23 °C. At this time allyl bromide (236 μL, 2.73 mmol) was added to the mixture, and it was heated to 60 °C for 5 h. The mixture was allowed to reach 23 °C and was carefully added over a stirring mixture of 4:1 EtOAc/brine (15 mL). The resulting white suspension was filtered through a short pad of Celite, washed with EtOAc, and organics were concentrated in vacuo. According to HPLC analysis of the crude product, 86% of the diastereomeric mixture corresponds to the major diastereoisomer. After column chromatography (3:2 hexane/EtOAc), the major isomer was isolated pure (>99:1 according to HPLC) as a white solid (532 mg, 72%). R_f = 0.26 (1:1 hexane/EtOAc); mp 31.6−32.9 °C; $[\alpha]^{20}_D$ = +76 (*c* 0.62 in $CHCl_3$); ^{1}H NMR (300 MHz, $CDCl_3$) δ 7.42−7.30 (m, 5H), 5.72 (dt, *J* = 16.6, 8.4 Hz, 1H), 5.26−5.01 (m, 4H), 4.88 (br s, 1H), 4.65 (br s, 1H), 4.03 (m, 1H), 2.94 (br s, 1H), 2.77 (t, *J* = 12.7 Hz, 1H), 2.53 (br s, 1H), 2.34 (dt, *J* = 13.9, 6.9 Hz, 1H), 2.02 (t, *J* = 12.7 Hz, 1H), 1.84−1.36 (m, 7H), 1.31−0.98 (2 x br s, 9H); ^{13}C NMR (101 MHz, $CDCl_3$) δ 156.0 (C), 137.0 (C), 135.4 (CH), 128.6 (CH), 128.1 (CH), 127.9 (CH), 117.6 (CH_2), 67.3 (CH_2), 55.8 (C), 53.3 (CH), 47.6 (CH), 39.4 (CH_2), 39.1 (CH_2), 36.4 (CH_2), 29.4 (CH_2), 25.6 (CH_2), 22.9 (CH_3), 19.3 (CH_2); IR (ATR) ν 3242, 3033, 2936, 1674, 1641, 1421, 1260, 1064 cm^{-1}; LRMS (EI) *m*/*z* (%) 350 ($M^+ - C_4H_8$, 3), 218 (10), 174 (29), 91 (100), 84 (19); HRMS (EI) *m*/*z* calcd for $C_{22}H_{34}N_2O_3S - C_4H_8$ 350.1664, found 350.1665; HPLC (Chiralcel AD-H column 25 cm × 0.46 cm, 95:5 hexane/*i*-PrOH, 1.0 mL min^{-1}, λ = 217 nm) t_R for major isomer 15.93 min, t_R other diastereoisomers 20.76−23.39 min.

(2*R*,2′*R*,*R*$_S$)-1-(Benzyloxicarbonyl)-2-[2′-*tert*-(butylsulfinamide)-4′-pentenyl]piperidine (3b). This compound was prepared from (R_S)-*tert*-butanesulfinamide (282 mg, 2.33 mmol) and compound **2** (610 mg, 2.34 mmol) following the same procedure described above for compound **3a**. According to HPLC analysis of the crude product, 95% of the diasteromeric mixture corresponds to the major diastereoisomer. After column chromatography (3:2 hexane/EtOAc) the major isomer was isolated pure (>99:1 dr according to HPLC) as a white solid (757 mg, 80%): R_f = 0.21 (1:1 hexane/EtOAc); mp 88.9−89.5 °C; $[\alpha]^{20}_D$ = −26 (*c* 0.80 in $CHCl_3$); ^{1}H NMR (300 MHz, $CDCl_3$) δ 7.48−7.29 (m, 5H), 5.73 (dt, *J* = 16.6, 8.4 Hz, 1H), 5.21−5.03 (m, 5H), 4.48 (br s, 1H), 4.07 (d, *J* = 13.3 Hz, 1H), 3.27 (dd, *J* = 12.8, 6.3 Hz, 1H), 2.89 (t, *J* = 12.5 Hz, 1H), 2.54−2.28 (m, 2H), 1.88−1.32 (m, 8H), 1.17 (br s, 9H); ^{13}C NMR (101 MHz, $CDCl_3$) δ 155.5 (C), 136.9 (C), 134.0 (CH), 128.6 (CH), 128.1 (CH), 128.0 (CH), 119.2 (CH_2), 67.2 (CH_2), 56.0 (C), 53.0 (CH), 47.8 (CH), 40.7 (CH_2), 39.6 (CH_2), 34.7 (CH_2), 27.8 (CH_2), 25.6 (CH_2), 22.7 (CH_3), 18.9 (CH_2); IR (ATR) ν 3219, 3032, 2947, 1664, 1642, 1438, 1267, 1056 cm^{-1}; LRMS (EI) *m*/*z* (%) 350 ($M^+ - C_4H_8$, 7), 218 (12), 174 (30), 91 (100), 84 (20); HRMS (EI) *m*/*z* calcd for $C_{22}H_{34}N_2O_3S - C_4H_8$ 350.1664, found 350.1680; HPLC (same conditions described for **3a**) t_R for major diastereoisomer 19.25 min, t_R for the minor diastereoisomer 17.88 min.

Tetraponerine T3. To a solution of compound **3a** (510 mg, 1.26 mmol) in THF (3.2 mL) was added dropwise aqueous 6 M HCl (628 μL, 3.77 mmol) at 0 °C under Ar. The reaction mixture was stirred for 1 h while reaching 23 °C. Aqueous 2 M NaOH (5 mL) was added to the mixture, and the free amine was extracted with EtOAc (3 × 10 mL) and washed with brine (1 × 10 mL). Organics were dried over $MgSO_4$, filtered, and concentrated under reduced pressure. The residue was then disolved in dry MeOH (24 mL), and Pd/C 10% (420 mg) was added to the mixture. The suspension was shacked under hydrogen atmosphere (4 atm) for 12 h at 23 °C and filtered though Celite, and the obtained solution was concentrated under reduced pressure. The residue (free diamine) was then dissolved in dry CH_2Cl_2 (13 mL), and K_2CO_3 (520 mg, 3.77 mmol) was added, followed by 4-bromobutanal[25] (285 mg, 1.89 mmol). The mixture was stirred at 23 °C for 4 h, after which time inorganic salts were removed by filtration. The filtrate was washed with aqueous $NaHCO_3$, followed by brine, and then dried over $MgSO_4$. Organics were concentrated under reduced pressure, and the residue was purified by column chromatography (96:4:0.05 CH_2Cl_2/MeOH/20% NH_4OH) to provide the desired product as an oil (151 mg, 54% from **3a**). R_f = 0.40 (9:1 CH_2Cl_2/MeOH); $[\alpha]^{20}_D$ = +35 (*c* 0.49 in $CHCl_3$) {lit.[5] $[\alpha]^{20}_D$ + 27 (*c* 0.07 in $CHCl_3$), lit.[9b] $[\alpha]^{20}_D$ = +35 (*c* 0.51 in $CHCl_3$)}; ^{1}H NMR (300 MHz, C_6D_6) δ 3.28 (dd, *J* = 4.8, 2.2 Hz, 1H), 3.20 (dd, *J* = 14.6, 7.4 Hz, 1H), 2.85−2.69 (m, 3H), 2.08−1.98 (m, 1H), 1.97−1.87 (m, 1H), 1.86−1.50 (m, 8H), 1.50−1.01 (m, 8H), 0.93 (t, *J* = 7.1 Hz, 3H); ^{13}C NMR (101 MHz, C_6D_6): δ = 75.7 (CH), 56.8 (CH), 52.8 (CH), 50.8 (CH_2), 50.7 (CH_2), 33.9 (CH_2), 33.2 (CH_2), 32.0 (CH_2), 30.4 (CH_2), 26.2 (CH_2), 25.1 (CH_2), 22.2 (CH_2), 20.7 (CH_2), 14.5 (CH_3); IR (ATR) ν 2952, 2927, 2869, 2803, 1455, 1390, 1354, 1157, 1129, 1113 cm^{-1}; LRMS (EI) *m*/*z* (%) 222 (M^+, 49), 221 (64), 194 (14), 193 (100), 180 (8), 179 (14), 152 (44), 138 (19), 137 (14), 124 (12), 110 (12), 97 (10), 96 (51), 84 (19); HRMS (EI) *m*/*z* calcd for $C_{14}H_{26}N_2$ 222.2096, found 222.2076; GC major peak (>98%) at 12.40 min.

Tetraponerine T4. It was prepared from **3b** (199 mg, 0.49 mmol) and 4-bromobutanal (111 mg, 0.74 mmol), following the same procedure described above for tetraponerine **T3**. The expected product was obtained as an oil (61 mg, 56% from **3b**). R_f = 0.43 (9:1 CH_2Cl_2/MeOH); $[\alpha]^{20}_D$ = +102 (*c* 0.34 in $CHCl_3$) {lit.[5] $[\alpha]^{20}_D$ = +94 (*c* 0.2 in $CHCl_3$), lit.[9b] $[\alpha]^{20}_D$ = +107 (*c* 1.16 in $CHCl_3$)}; ^{1}H NMR (400 MHz, C_6D_6) δ 3.16 (td, *J* = 8.2, 2.2 Hz, 1H), 2.83 (d, *J* = 8.1 Hz, 1H), 2.35 (t, *J* = 6.3 Hz, 1H), 2.13 (ddd, *J* = 10.7, 7.1, 3.4 Hz, 1H), 2.04 (dd, *J* = 15.9, 8.5 Hz, 1H), 1.86−1.55 (m, 7H), 1.55−1.05 (m, 11H), 0.88 (t, *J* = 7.1 Hz, 3H); ^{13}C NMR (101 MHz, C_6D_6) δ 86.0 (CH), 63.3 (CH), 61.4 (CH), 51.9 (CH_2), 49.2 (CH_2), 37.9 (CH_2), 37.3 (CH_2), 33.2 (CH_2), 30.0 (CH_2), 26.5 (CH_2), 25.5 (CH_2), 20.8 (CH_2), 19.3 (CH_2), 15.3 (CH_3); IR (ATR) ν 2930, 2870, 2789, 1646, 1454, 1377, 1337, 1190, 1157, 1025 cm^{-1}; LRMS (EI) *m*/*z* (%) 222 (M^+, 49), 221 (100), 194 (14), 193 (98), 180 (15), 179 (15), 152 (30), 151 (20), 138 (22), 137 (14), 124 (14), 110 (13), 96 (35), 84 (19); HRMS (EI) *m*/*z* calcd for $C_{14}H_{26}N_2$ 222.2096, found 222.2064; GC major peak (>98%) at 12.74 min.

Computational Details. All of the 24 structures of Charts 1 and 2 were built as explained in the text and were initially optimized using a MM2 force field before being submitted to density functional theory calculations (DFT). DFT calculations of the structures,[26] energies, and harmonic vibrational analysis were carried out using the Becke−Lee−Yang−Parr (B3LYP) exchange-correlation functional.[27] We relied on the widely used B3LYP functional, the performance of which was reviewed recently with a collection of molecules of biological relevance on the basis of the reported errors in barrier height energy (for singlet transition states) and conformational energies,[28] and also specifically for this functional with a larger set of neutral, closed-shell organic molecules containing C, H, N, and O atoms, on the basis of the isomerization energies for nitrogen-containing molecules.[29] Important correlation energy corrections due to noncovalent, medium-range interactions are not expected.[30] The geometries of the isolated species have been fully optimized in the gas phase using the split valence triple-ζ 6-311+G (2d,p) basis set.[31] When both polarization and diffuse functions are used, an improvement of the isomerization energies of amines was reported for this functional.[29] In addition a double set of polarization functions was used to get a better description of the inversion barriers at the nitrogen. A preliminary study with a typical double-ζ 6-31G (d) basis set was also carried out to test the level of convergence of the energies with the size of the base, which was considered adequate for our purposes. Analytic second derivative calculations, which yield the harmonic frequencies, were performed on the optimized geometries at the same level of theory to ensure that the optimized geometries were true minima and to provide corrections for the zero-point energy (ZPE) effects. The Hessian matrices of the optimized geometries had only positive eigenvalues. The activation barriers were located using the synchronous transit-guided quasi-Newton (STQN) method,[32] requested both with the QST2 (two input structures) and QST3 (three input structures) formalism. Frequency analysis was carried out subsequently to make sure that true first order saddle points were located, giving rise to a one negative eigenvalue. The calculations were carried out with the GAUSSIAN 09 suite of programs.[33]

■ ASSOCIATED CONTENT

Supporting Information

Copies of ^{1}H and ^{13}C NMR spectra for all new or relevant compounds prepared, as well as HPLC traces of **3a**/**3b** and GC−MS for **T3** and **T4**, are provided. Optimized geometries and zero point energies (Ha), as well as thermodynamic data for all calculated structures by DFT is also given. This material is available free of charge via the Internet at http://pubs.acs.org.

■ AUTHOR INFORMATION

Corresponding Author

*E-mail: josecarlos.gonzalez@ua.es; aguijarro@ua.es.

Notes

The authors declare no competing financial interest.

■ ACKNOWLEDGMENTS

We thank the Spanish Ministerio de Ciencia e Innovación (Grant No. CTQ2007-65218, Consolider Ingenio 2010-CSD-2007-00006 and CTQ2011-24165), the Generalitat Valenciana (Grant No. PROMETEO/2009/039 and FEDER), and the University of Alicante for their financial support. I.B. also thanks the Generalitat Valenciana for a predoctoral fellowship (ACIF/2011/159).

■ DEDICATION

Dedicated to the memory of Professor Balbino Mancheño.

■ REFERENCES

(1) Braekman, J. C.; Daloze, D.; Pasteels, J. M.; Vanhecke, P.; Declercq, J. P.; Sinnwell, V.; Francke, W. *Z. Naturforsch.* **1987**, *42c*, 627−630.

(2) Renson, B.; Merlin, P.; Daloze, D.; Braekman, J. C.; Roisin, Y.; Pasteels, J. M. *Can. J. Chem.* **1994**, *72*, 105−109.

(3) Devijver, C.; Braekman, J. C.; Daloze, D.; Pasteels, J. M. *Chem. Commun.* **1997**, 661−662.

(4) Yue, C.; Royer, J.; Husson, H.-P. *J. Org. Chem.* **1990**, *55*, 1140−1141.

(5) Macours, P.; Braekman, J. C.; Daloze, D.; Pasteels, J. M. *Tetrahedron* **1995**, *51*, 1415−1428.

(6) Structures of **T5** and **T6** were also confirmed by chemical synthesis in: Devijver, C.; Macours, P.; Braekman, J. C.; Daloze, D.; Pasteels, J. M. *Tetrahedron* **1995**, *51*, 10913−10922.

(7) Kem, W. R.; Wildeboer, K.; LeFrancois, S.; Raja, M.; Marszalec, W.; Braekman, J. C. *Cell Mol. Neurobiol.* **2004**, *24*, 535−551.

(8) Rouchaud, A.; Braekman, J. C. *Eur. J. Org. Chem.* **2009**, 2666−2674.

(9) For selected syntheses of enantioenriched tetraponerines, see: (a) Chongwei, Y.; Gauthier, I.; Royer, J.; Husson, H.-P. *J. Org. Chem.* **1996**, *61*, 4949−4954. (b) Takahata, H.; Kubota, M.; Ikota, N. *J. Org. Chem.* **1999**, *64*, 8594−8601. (c) Stragies, R.; Blechert, S. *J. Am. Chem. Soc.* **2000**, *122*, 9584−9591. (d) Airiau, E.; Girard, N.; Pizzeti, M.; Salvadori, J.; Taddei, M.; Mann, A. *J. Org. Chem.* **2010**, *75*, 8670−8673.

(10) The use of 4-bromobutanal was already reported for the synthesis of (±)-**T8** using a different approach: Barluenga, J.; Tomás, M.; Kouznetsov, V.; Rubio, E. *J. Org. Chem.* **1994**, *59*, 3699−3700.

(11) (a) González-Gómez, J. C.; Medjahdi, M.; Foubelo, F.; Yus, M. *J. Org. Chem.* **2010**, *75*, 6308−6311. (b) González-Gómez, J. C.; Foubelo, F.; Yus, M. *Org. Synth.* **2012**, *89*, 88−97.

(12) Bosque, I.; González-Gómez, J. C.; Foubelo, F.; Yus, M. *J. Org. Chem.* **2012**, *77*, 780−784; Corrigenda: *J. Org. Chem.* **2012**, *77*, 4190.

(13) Yu, W.; Mei, Y.; Kang, Y.; Hua, Z.; Jin, Z. *Org. Lett.* **2004**, *6*, 3217−3219.

(14) This was expected since the $d_{C\text{-}N}$ (C_5−N_4 bond lengths) are customarily some 4−9% shorter than the $d_{C\text{-}C}$ (C_5−C_6 bond lengths).

(15) The actual optimized geometries, absolute energies, zero-point energies, enthalpies, and free energies under standard conditions (1 atm, 298.15 K) are available for all of the structures in the Supporting Information.

(16) The accuracy of these results has been estimated by comparison with a preliminary study at the B3LYP/6-31G (d) level. Both calculations have identical profiles, with an average absolute deviation of the energies in the whole set of ±0.4 and ±0.7 kcal mol^{-1} for **T3** and **T4** respectively.

(17) Analogues of this configuration have been apparently used to represent the structure of some tetraponerines in the past. See: Kim, J. T.; Gevorgyan, V. *Org. Lett.* **2002**, *4*, 4697−4699 (Supporting Information).

(18) For a sample of 16 structures from Charts 1 and 2, only those with nondeformed chair geometries in rings A and B were included.

(19) (a) *NBO Version 3.1*; Glendening, E. D.; Reed, A. E.; Carpenter, J. E.; Weinhold, F. (b) Reed, A. E.; Weinstock, R. B.; Weinhold, F. *J. Chem. Phys.* **1985**, *83*, 735−46. (c) Reed, A. E.; Weinhold, F. *J. Chem. Phys.* **1985**, *83*, 1736−40.

(20) A detailed account of these specific interactions for the main configurations (those in Figure 2) can be found in the Supporting Information S27−S28.

(21) Gribble, G. W.; Nelson, R. B. *J. Org. Chem.* **1973**, *38*, 2831−2834.

(22) We shall limit the description to the structures within 3 kcal mol^{-1} from the absolute minimum.

(23) We determined this ΔG° from the calculated standard free energies taking into consideration that both T3 and T4 are actual mixtures of conformations:

$$\Delta G^{\circ} = -RT[\ln \sum_{i} e^{-G_i^{\circ}(\mathbf{T4})/RT} - \ln \sum_{j} e^{-G_j^{\circ}(\mathbf{T3})/RT}]$$

(24) Interestingly, the nitrogen inversion for **T4** is ca. 3 kcal mol^{-1} higher than for **T3**. During the inversion process, the C_3 has to overcome a gauche interaction with the propyl group in **T4**, which is missing in **T3**.

(25) 4-Bromobutanal is commercially available, but we prepared it by DIBAL-H reduction of the corresponding methyl esther.

(26) (a) Hohenberg, P.; Kohn, W. *Phys. Rev.* **1964**, *136*, B864−B871. (b) Kohn, W.; Sham, L. *J. Phys. Rev.* **1965**, *140*, A1133−A1138.

(27) (a) Becke, A. D. *J. Chem. Phys.* **1993**, *98*, 5648−5652. (b) Stephens, P. J.; Devlin, F. J.; Chablowski, C. F.; Frisch, M. J. *J. Phys. Chem.* **1994**, *98*, 11623−11627.

(28) Riley, K. E.; Op't Holt, B. T.; Merz, K. M., Jr. *J. Chem. Theory Comput.* **2007**, *3*, 407−433.

(29) Tirado-Rives, J.; Jorgensen, W. L. *J. Chem. Theory Comput.* **2008**, *4*, 297−306.

(30) Zhao, Y.; Truhlar, D. G. *J. Chem. Theory Comput.* **2007**, *3*, 286−300.

(31) Krishnan, R.; Binkley, J. S.; Seeger, R.; Pople, J. A. *J. Chem. Phys.* **1980**, *72*, 650−654.

(32) Peng, C.; Ayala, P. Y.; Schlegel, H. B.; Frisch, M. J. *J. Comput. Chem.* **1996**, *17*, 49−56.

(33) Frisch, M. J.; Trucks, G. W.; Schlegel, H. B.; Scuseria, G. E.; Robb, M. A.; Cheeseman, J. R.; Scalmani, G.; Barone, V.; Mennucci, B.; Petersson, G. A.; Nakatsuji, H.; Caricato, M.; Li, X.; Hratchian, H. P.; Izmaylov, A. F.; Bloino, J.; Zheng, G.; Sonnenberg, J. L.; Hada, M.; Ehara, M.; Toyota, K.; Fukuda, R.; Hasegawa, J.; Ishida, M.; Nakajima, T.; Honda, Y.; Kitao, O.; Nakai, H.; Vreven, T.; Montgomery, J. A.; Jr.; Peralta, J. E.; Ogliaro, F.; Bearpark, M.; Heyd, J. J.; Brothers, E.; Kudin, K. N.; Staroverov, V. N.; Kobayashi, R.; Normand, J.; Raghavachari, K.; Rendell, A.; Burant, J. C.; Iyengar, S. S.; Tomasi, J.; Cossi, M.; Rega, N.; Millam, J. M.; Klene, M.; Knox, J. E.; Cross, J. B.; Bakken, V.; Adamo, C.; Jaramillo, J.; Gomperts, R.; Stratmann, R. E.; Yazyev, O.; Austin, A. J.; Cammi, R.; Pomelli, C.; Ochterski, J. W.; Martin, R. L.; Morokuma, K.; Zakrzewski, V. G.; Voth, G. A.; Salvador, P.; Dannenberg, J. J.; Dapprich, S.; Daniels, A. D.; Farkas, O.; Foresman, J. B.; Ortiz, J. V.; Cioslowski, J. Fox, D. J. *Gaussian 09, Revision A.02*; Gaussian, Inc.: Wallingford, CT, 2009.